PAPER

Externally tunable multichannel filtering applications of organic material based 1D magnetic cold-plasma photonic crystals

S. K. Awasthi,[a] Alireza Aghajamali,[b] A. M. Mohamed,[c] Z. S. Matar,[d] A. F. Amin[e] and Arafa H. Aly [ID] *[c]

In the present research work, we employed the transfer matrix method (TMM) in addition to MATLAB software to examine the transmission properties of various organic-based one-dimensional (1D) magnetic cold-plasma photonic crystals (MCPPhCs). The proposed structures were found to be made up of periodic layers of organic materials and magnetic cold-plasma (MCP) at normal incidence. An external magnetic field (B) polarized in right-hand (RH) and left-hand (LH) configurations was applied on 1D MCPPhCs. In this study, four organic materials, namely pentane, hexane, heptane, and octane, were chosen to design four 1D photonic crystals (PCs), named as PC_1 (pentane-MCP), PC_2 (hexane-MCP), PC_3 (heptane-MCP), and PC_4 (octane-MCP). Our results indicated that the central frequency of the resonant peaks of unit transmission inside the photonic band-gap (PBG) of the respective organic PCs could be tuned towards the higher or lower frequency side by applying B polarized in RH and LH configurations, respectively. We also studied the effect of the period number N to produce closely spaced N-1 transmission channels of unit transmission inside the PBG of all four organic PCs. By increasing the period number N we could increase the number of transmission channels inside the PBG as per our desire. These multiple resonant peaks of unit transmission inside PBG could be easily modulated inside the PBG to accommodate new frequencies by applying B polarized in either RH or LH configurations, respectively. Moreover, our results showed that under the RH configuration, increasing B resulted in a shifting of the resonant peak towards the higher frequency side with a reduction in its full width half maximum (FWHM), whereas the findings were the opposite in the case of increasing B under the LH configuration. These findings may be beneficial for designing externally tuneable organic chemical sensors in the microwave frequency region.

1. Introduction

The one-dimensional (1D) photonic structure has received great attention compared to two-dimensional (2D) and three-dimensional (3D) photonic crystals (PCs) due to their special characteristics, such as ease of manufacture, low cost, and simple architecture.[1–5] The foremost beauty of such structures is their special ability to exhibit unique optical, mechanical, and electrical properties when interacting with electromagnetic waves (EMWs) due to the existence of a photonic band-gap (PBG), which controls the propagation of EMWs passing through them. PBG indicates the frequency region in which EMW propagation is forbidden through the structure due to the destructive interference from EMWs reflected from the interface of the constituent material layers. The disturbance in the periodicity of conventional PCs may result in a sharp defect mode of unit transmission inside PBG due to photon confinement, which opens a new horizon in the field of photonic biosensing and engineering.[6] The position and intensity of the defect mode in addition to the width of PBG are highly influenced by varying the structural parameters, such as the thickness of the constituent material layers of the structure, angle of incidence, refractive index of the constituent materials, and state of polarization of incident light. The optical characteristics of the defect mode and PBG of 1D PCs can be easily manipulated to control their reflection, absorption, and transmission responses. This tremendous ability of 1D PCs with defects may be exploited for enormous photonic applications, such as biosensors, optical switches, optical splitters, and optical filters.[7–10]

[a]*Department of Physics and Material Science and Engineering, Jaypee Institute of Information Technology, Noida 201304, U. P, India*

[b]*School of Molecular Sciences, The University of Western Australia, Perth, WA 6009, Australia*

[c]*TH-PPM Group, Physics Department, Faculty of Sciences, Beni-Suef University, Beni Suef, 62514, Egypt. E-mail: arafa.hussien@science.bsu.edu.eg; arafaaly@aucegypt.edu*

[d]*Faculty of Applied Science, Department of Physics, Umm Al-Qura University, Mecca 24382, Saudi Arabia*

[e]*Faculty of Technology and Education, Beni-Suef University, Beni Suef 62521, Egypt*

Recently, researchers have shown keen interest in developing PC-based devices composed of gyroidal, metamaterial, super-conductor, liquid crystal, metal, nanocomposite materials, *etc.* for a variety of potential applications, such as omnidirectional mirrors, all-optical switches, high-sensitivity biosensors, PBG waveguides, and tuneable filters.[11] Hojo and Mase (2004) suggested a new type of PC composed of plasma. They called this PC a plasma photonic crystal (PPC). They found a tuneable PBG in the microwave frequency region that could be tuned by changing the plasma parameters, like the plasma density, collision frequency, and electron density.[12] In order to make the PBG characteristic of a PPC externally tuneable, nowadays magnetic cold-plasma has attracted lot of interest due to the external magnetic field-dependent behaviour of the electric permittivity of magnetic cold-plasma (MCP). In the presence of an external magnetic field (B) polarized in right-hand (RH) and left-hand (LH) configurations, the gyro-effective frequency of MCP exhibits positive and negative values, respectively.[13] Apart from the external magnetic field polarized in the RH and LH configurations, the refractive index of MCP can also be effectively managed by other plasma parameters, like the collision frequency and electron density.[14] The aforementioned properties of MCP materials make them suitable for designing externally tuneable PCs in the microwave frequency region contrary to conventional PCs. The first conceptual realization of a 1D PC composed of an MCP material was also given by Hojo and his coworkers.[15] In that work, they examined the tuneable PBG properties of a 1D PC consisting of an MCP material. The captivating optical characteristics of PCs consisting of an MCP material have become a central aspect of the current plasma photonic research. Zaky *et al.* proposed a novel way to detect the refractive index of various bio-analytes with the help of a 1D PC composed of periodic layers of MCP material in the presence of a B polarized in RH and LH configurations.[16] Awasthi *et al.* investigated the tuneable multichannel filtering application of 1D magnetic cold-plasma PCs by examining the transmission and reflection properties in the presence of an external magnetic field polarized in both RH and LH configurations in the microwave frequency region.[17] Arafa *et al.* studied the tuneable properties of a 1D PC with an MCP defect layer.[18] Nevertheless, a large number of research studies based on 1D PCs based on MCP materials have been carried out to investigate magnetic field-governed multichannel filtering applications in the microwave region, but still the biosensing and organic material sensing applications of 1D PCs composed of MCP materials have not yet been explored.

The present research work highlights the tuneable multi-channel filtering properties of 1D PCs consisting of organic materials and MCP and has certain uniqueness. Nowadays, organic compounds are considered to be one of the most essential chemicals that are widely used in our daily life, such as chemical industries, food industry, medical research, and biochemistry. The undesirable direct release of chemical waste from such industries may pollute our water reservoirs and poses a major threat to our environment.[19] Moreover the presence of organic compounds in the human body may cause several incurable diseases in the human body. Thus, it is essential to develop conventional as well as unconventional techniques for the detection of compounds in a timely manner to save our society and environment from the adverse effects of organic compounds. At present, there are a several ways extending from chemical gas sensors to terahertz (THz) spectroscopy to detect these compounds, such as quartz crystal microbalance, the electronic nose, and solvent response materials. The present study deals with the multichannel filtering applications of 1D PCs composed of organic materials and MCP in the presence of an external magnetic field polarized in RH and LH configurations. This idea may further be used for the development of organic-material-detection technology based on PCs due to the excellent sensing capabilities of photonic structures.[20–23]

In this study, we examined the tuneable multichannel properties of four 1D PCs composed of four different organic materials, namely pentane, hexane, heptane, and octane, along with MCP material separately in the presence of B polarized in RH and LH configurations. The effect of the period number N on the multichannel filtering property in the presence B polarized in RH and LH configurations was also examined to increase the number of resonant peaks inside the PBG of all four 1D PCs containing different organic materials. The proposed photonic structures could be easily realized with the help of existing fabrication technologies. The architecture of the proposed work is described in Section 2, which also deals with the theoretical modelling and formulation of the design. The results and discussion of the work are discussed in Section 3. Finally, Section 4 presents the conclusions.

2. Theoretical modelling and formulation

In this section, we describe the theoretical formation pertaining to the proposed design. We considered 1D PCs $(AB)^N$ composed of different organic materials and MCP. Here, the letters A and B represent the organic and MCP materials used in the design, respectively. The period number of the proposed design is represented by N. The entire structures were kept in the air. The thickness, permittivity, and permeability of the jth layers of 1D PC $(AB)^N$ are represented as d_j, ε_j, and μ_j respectively. Here, j = A, B is used for layers A and B of the design (Fig. 1).

The transfer matrix formulation was used to investigate the transmission properties of the proposed 1D PCs based on the organic materials pentane, hexane, heptane, and octane. The total transfer matrix representing the entire structure takes the form of:[13–18]

$$M = \begin{pmatrix} m_{11} & m_{12} \\ m_{21} & m_{22} \end{pmatrix} = D_0^{-1} \left(\prod_{j=1}^{N} D_j P_j D_j^{-1} \right) P_s \qquad (1)$$

where the subscripts 0 and S are used for the incident and exit media just behind the structure, respectively, and the notations P_j and D_j represent the propagation and dynamic matrixes of jth layer of thickness d_j of the structure, as defined in eqn (2) and (3), respectively.

$$P_j = \begin{pmatrix} e^{-ik_{jz}d_j} & 0 \\ 0 & e^{ik_{jz}d_j} \end{pmatrix} \qquad (2)$$

Here, the z component of the wave number k under normal incidence is given as $k_{jz} = (\omega/c)n_j$, where n_j, ω, and c represent the refractive index, wave frequency, and speed of the wave in free space inside the jth layer, respectively. According to eqn (1), the dynamic matrix of layer j under normal incidence is defined as:

$$D_j = \begin{pmatrix} 1 & 1 \\ n_j & -n_j \end{pmatrix} \qquad (3)$$

The transmission coefficient t of the 1D PC $(AB)^N$ at normal incidence is given by $t = 1/m_{11}$, where m_{11} is given in eqn (1). The transmittance T of a 1D MCPPhC can be computed with the help of the relation given in eqn (4) below.

$$T = \frac{n_s \cos \theta_s}{n_0 \cos \theta_0} |t^2|. \qquad (4)$$

Now, let us describe the refractive index of the organic and magnetized cold-plasma materials used in this work. As mentioned earlier, in this study, we considered four different organic materials, namely pentane, hexane, heptane, and octane, to design the materials PC1 to PC4. The frequency-dependent refractive indices of these organic materials are given by ref. 19 as:

$$n_{pentane} = 1.35254253 - \frac{(3.59105 \times 10^{-3})}{\omega} + \frac{(4.17342 \times 10^{-3})}{\omega^2}, \qquad (5)$$

$$n_{hexane} = 1.34830572 - \frac{(3.93237 \times 10^{-3})}{\omega} + \frac{(4.42005 \times 10^{-3})}{\omega^2}, \qquad (6)$$

$$n_{heptane} = 1.38248838 - \frac{(4.05375 \times 10^{-3})}{\omega} + \frac{(4.58433 \times 10^{-3})}{\omega^2}, \qquad (7)$$

$$n_{octane} = 1.39260498 - \frac{(4.48963 \times 10^{-3})}{\omega} + \frac{(4.79591 \times 10^{-3})}{\omega^2}. \qquad (8)$$

In addition, the frequency and magnetic field-dependent refractive index of MCP is given by $n_{MCP} = (\varepsilon_{MCP}(\omega))^{1/2}$, where ε_{MCP} represents frequency-dependent complex permittivity of MCP. It is defined as:[14–17]

$$\varepsilon_{MCP}(\omega) = 1 - \frac{\omega_{pe}^2}{\omega^2 \left(1 - i\dfrac{\gamma}{\omega} \mp \dfrac{\omega_{le}}{\omega}\right)}. \qquad (9)$$

where the symbols ω, ω_{pe}, ω_{le} and γ are used to point out the angular, plasma, gyro, and effective collision frequencies of a magnetic cold-plasma material, respectively. The symbol $\mp$ in eqn (9) represents the external magnetic field polarized in the RH and LH configurations respectively. The ω_{pe} and ω_{le} frequencies can be calculated with the help of eqn (10) and (11), respectively, as:

$$\omega_{pe} = \frac{n_e e^2}{m\varepsilon_0} \qquad (10)$$

$$\omega_{le} = \frac{e\mathbf{B}}{m} \qquad (11)$$

where n_e, e, and m are the electron density, charge, and mass of electron, respectively.

3. Numerical results and discussion

We examined the transmission characteristics of our proposed 1D MCPPhC $(AB)^N$ consisting of periodic layers of organic and magnetic cold-plasma materials with the help of TMM and MATLAB software. The thicknesses of layers A (organic material) and B (magnetized cold-plasma) of the proposed structure were selected as $d_1 = 14$ mm and $d_2 = 10$ mm, respectively. The numerical values of the different parameters of magnetic cold-plasma were chosen as $\gamma = 2 \times 10^7$ Hz, $m_0 = 9.31 \times 10^{-31}$ kg, and $n_e = 8 \times 10^{17}$ m^{-3} to carry out the simulations in this work.

In the first part of this study, we investigated the behaviour of the permittivity function of magnetic cold-plasma dependent on the frequency, which was varied from 2.5 GHz to 7.0 GHz in the presence of an external magnetic field under right-hand and left-hand polarization configurations. Fig. 2 shows the frequency-dependent behaviour of the real and imaginary parts of the permittivity function of magnetic cold-plasma in the presence of B polarized in both RH and LH configurations. Fig. 2(a) and (b) show the behaviour of the real and imaginary parts of the permittivity function of magnetic cold-plasma dependent on the frequency in the presence of B under the RH configuration. For this purpose, we varied the value of B as 0T, 0.03T, 0.05T, and 0.07T under the RH configuration. It can be observed from Fig. 2(a) that as B changed between 0T to 0.07T, the real part of the frequency-dependent permittivity function of the plasma layer Re(ε_p) became more negative. Thus, the magnetic cold-plasma layer could be used as tuneable epsilon negative material, which is the class of a single negative medium in the frequency range 2.5 GHz to 7.0 GHz. This tunability was prominent towards lower frequency but became stagnant towards the higher frequency side as B changed from 0T to 0.07T under the RH configuration. On the other hand, the frequency-dependent behaviour of the imaginary part of the permittivity function of plasma Imag(ε_p) under the influence of $B = 0$T, 0.03T, 0.05T, and 0.07T in the RH configuration is plotted in Fig. 2(b), and shows that the increase in B also increased the loss associated with the magnetic cold-plasma layer. These losses were prominent towards the lower frequency side but became negligible towards the higher side of the frequency region, which varied from 2.5 GHz to 7.0 GHz under the influence of B in the RH configuration. The frequency-dependent behaviour of Re(ε_p) and Imag(ε_p) under the influence of B in the LH configuration was also examined in this study, as shown in Fig. 2(c) and (d), respectively. Fig. 2(c) and (d) show that the increase in B from 0T to 0.07T under the LH configuration not only increased the negative value of Re(ε_p) of the magnetic cold-plasma but also lowered the value of
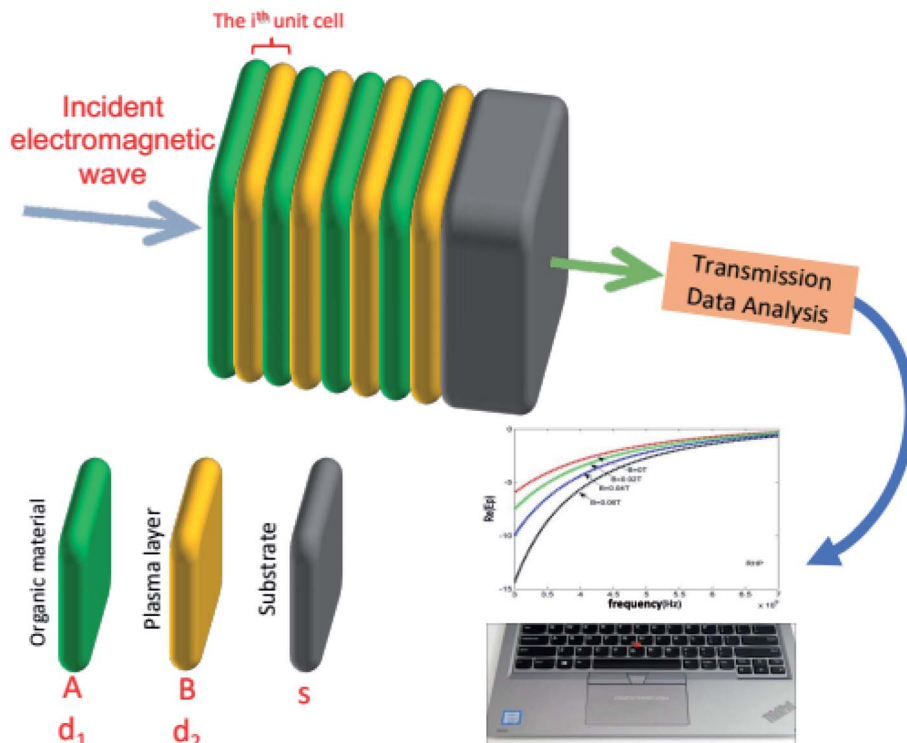
Fig. 1 Architecture of the proposed 1D PCs $(AB)^N$ composed of organic materials and magnetic cold-plasma under normal incidence. Here, the letters A and B are used to represent the periodic layers of organic and MCP materials, respectively. The layers A and B of thicknesses d_1 and d_2 are depicted by green and yellow colours, respectively. The grey layer shows the substrate material, which was air in our case.

$\text{Imag}(\varepsilon_p)$, which was a measure of the losses associated with the magnetic cold-plasma. This behaviour was prominent towards the lower frequency side but almost stagnant towards the high frequency side. Thus, the magnetic field-dependent behaviour of $\text{Re}(\varepsilon_p)$ and $\text{Imag}(\varepsilon_p)$ of magnetic cold-plasma was opposite in nature under RH and LH configurations, but in both configurations, the plasma behaved as a tuneable dispersive epsilon negative media in the GHz frequency region, which is in the class of a single negative medium. In the present work, we used this externally tuneable property of the magnetic cold-plasma layer to study the multichannel tuneable filter
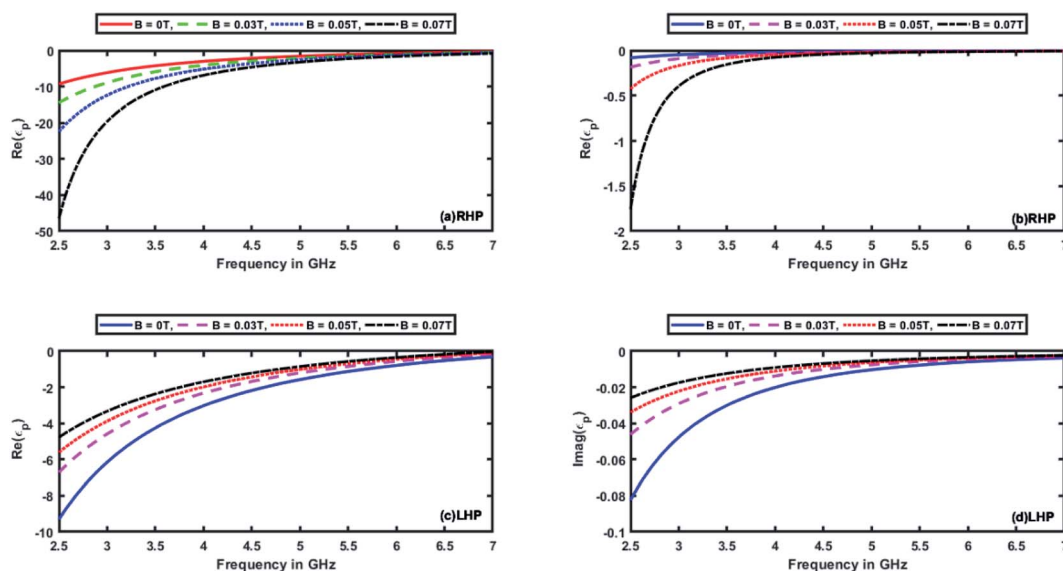

Fig. 2 Real and imaginary parts of the frequency-dependent permittivity function of MCP in the presence of $B = 0T$, 0.03T, 0.05T, and 0.07T under a RH configuration (a) and (b) and under a LH configuration (c) and (d), respectively.

properties of 1D PCs composed of alternate layers of organic material and magnetic cold-plasma.

Next, we investigated the transmission properties of four different 1D MCPPhCs composed of pentane, heptane, hexane, and octane, as well as magnetic cold-plasma layers to form PC_1, PC_2, PC_3, and PC_4, respectively. The period number of each PC was fixed to $N = 2$. The transmission spectrum of each PC was simulated between the frequency range 3.5 GHz to 5 GHz, as shown in Fig. 3(a) and (b), corresponding to $B = 0.03T$ in the RH and LH configurations, respectively. Fig. 3(a) shows four resonant peaks in the transmission spectra of the 1D PCs PC_1 to PC_4 under $B = 0.03T$ in the RH configuration. It could be observed that the position of the resonant peaks inside the PBG was different for the PCs composed of different organic materials due to their different frequency-dependent responses of the permittivity function, as discussed in eqn (5)–(8). For example, the transmission spectrum of 1D MCPPhC composed of the organic material hexane showed a resonant peak represented by

a dashed–dotted magenta line in Fig. 3(a). This resonant peak appeared around 4.5 GHz, while the position of the resonant peak was red-shifted for MCPPhC composed of the organic material octane. The transmission spectra of all four organic PCs as discussed above were also investigated at $B = 0.03T$ under the LH configuration. The results are plotted in Fig. 3(b) below. It can be observed that at $B = 0.03T$ under the LH configuration case, the position of the resonant peaks associated with the different organic PCs moved towards the lower frequency side and also their FWHM increased in comparison with the results under the RH configuration. It should also be noted that, in both cases, the energy associated with all the peaks was 100%, as evident from Fig. 3(a) and (b). The maximum transmittance of the resonant peaks was independent of the nature of the organic layer as well as B under both the RH and LH configurations. Thus, the main difference between the behaviour of the different organic PCs in the presence of B polarized in RH and LH cases was that in the LH case, the resonant peaks not only appeared at the lower frequency side but also became wider in contrast to the findings under the RH case. Thus, the external magnetic field polarized in RH and LH configurations can be used to tune the position of the resonant peak associated with the 1D PCs composed of different organic materials to either the higher or lower frequency side, respectively, and thus can overcome the difficulties associated with the angle dependent tuning of resonant peaks as discussed in ref. 13.

Further, we examined the transmittance response of the proposed 1D MCPPhC composed of pentane in the presence of B varying from $B = 0T$ to $0.07T$ and polarized in RH and LH configurations, as shown in Fig. 4(a) and (b), respectively, for a fixed value of $N = 2$. Fig. 4(a) shows that as B increased from 0T to 0.07T under the RH configuration, the resonant peak started to move towards the higher side of frequency inside the PBG and also its FWHM was reduced significantly. Additionally, when changing the B for 0T to 0.07T under the LH configuration, the resonant peak associated with the 1D MCPPhC composed of pentane started to move towards the lower frequency side and also its FWHM increased, as shown in Fig. 4(b). Thus, the application of B polarized in RH and LH configurations can be used to tune the position of the resonant peak inside the PBG at $B = 0T$ to either higher and lower frequency sides by changing B polarized in RH and LH configurations, respectively. Besides this, the FWHM of the defect mode can also be increased or decreased in order to improve the performance of the design suitable for organic material-based sensing applications. Further, we investigated the effect of changing the period number N from 2 to 3, 4, 5, and 6 of the photonic structure composed of the organic material pentane at a fixed value of $B = 0.02T$ under the RH configuration on the transmission properties of the MCPPhC. The results are shown just below, and in Fig. 4(a) corresponding to $N = 2, 3, 4, 5,$ and 6. It could be observed that at $N = 2$, there existed only one resonant peak of 100% transmission inside the PBG extending from 2.5 GHz to 7.0 GHz located between the frequency range 3.8 GHz to 5.2 GHz. At $N = 3$, there existed two resonant peaks of unit transmission, which were centred at either side of the
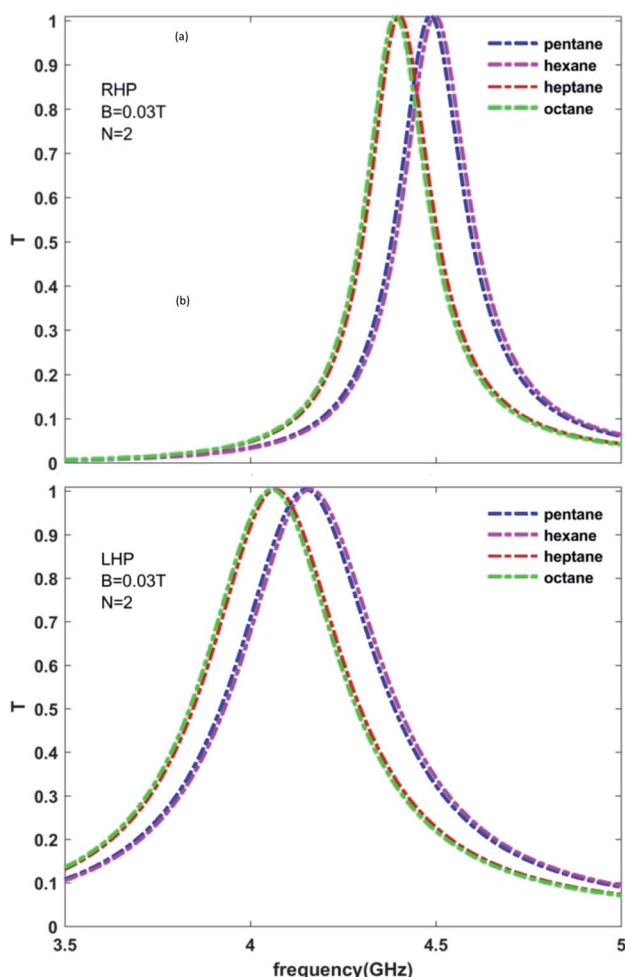

Fig. 3 Transmission response of the proposed 1D MCPPhCs under normal incidence of period number $N = 2$. The blue, purple, red, and green coloured dashed–dotted lines represent the transmission response of the 1D MCPPhCs composed of the organic materials pentane, hexane, heptane, and octane, respectively, in the presence of $B = 0.03T$ polarized in (a) RH and (b) LH configurations.
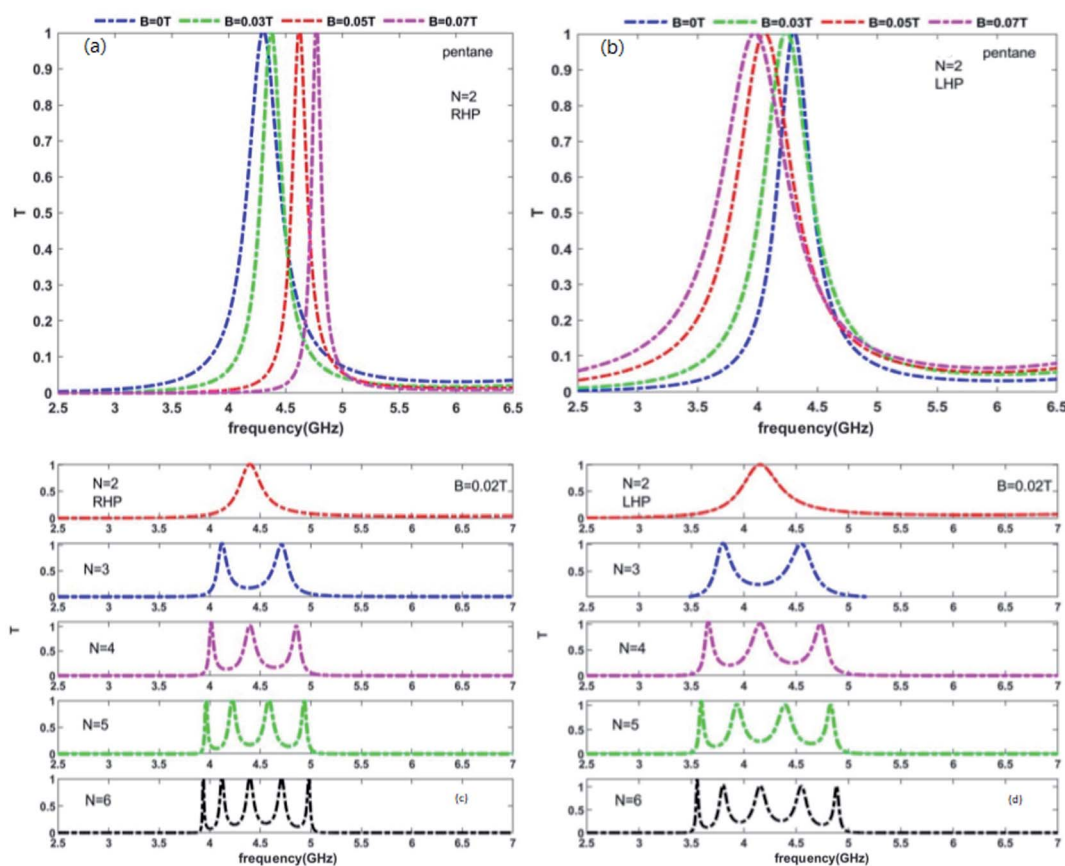
Fig. 4 Effect of the external magnetic field (a and b) and the number of lattice constants (c and d) on the position and number of resonance peaks for both right- and left-hand polarizations plasma layer and when the organic layer is pentane.

resonant peak corresponding to $N = 2$ between the frequency range of 3.8 GHz to 5.2 GHz. The same observation could be drawn corresponding to $N = 4$ to $N = 6$. Thus we can conclude that there were N-1 resonant peaks of unit transmission for a given N between the frequency range of 3.8 GHz to 5.2 GHz. Moreover the central frequency of each resonant peak inside the PBG extending from 2.5 GHz to 7.0 GHz was different for $N = 2$ to $N = 7$. For MCPPhC having even values of N, there existed an odd number of resonant peaks, whereas for MCPPhCs with an odd number of N there existed an even number of resonant peaks of different central frequencies. Thus the number of resonant peaks could be increased by increasing the period number N of the structure. The application of $B = 0.02T$ polarized in the LH configuration resulted in a slight shifting of the resonant peaks towards the lower frequency side, as shown in the figures drawn for $N = 2$ to $N = 7$ just below Fig. 4(b). This movement was pronounced for the peaks near to 2.5 GHz, whereas the peaks close to 7.0 GHz were almost stagnant. The other findings were similar to the RH configuration. The FWHM of the resonant peaks dependent upon N either decreased or increased depending on the RH or LH configuration of B.

Next, we investigated the similar findings of 1D MCPPhC composed of hexane and heptane under the influence of B polarized in RH and LH configurations. The period number N of both 1D MCPPhCs composed of hexane and heptane was fixed

at 2. The transmission spectra of the 1D MCPPhCs composed of the organic materials hexane and heptane in the presence of B, which varied from 0T to 0.07T, under RH and LH configurations are shown in Fig. 5 and 6, respectively. The findings of Fig. 5 and 6 are similar to the findings of Fig. 4 as discussed above, only with a difference in that the resonance peak appeared slightly at the higher and lower frequency sides corresponding to MCPPhC composed of hexane and heptane, respectively. The other findings were similar to the case of pentane as discussed above.

Finally, let us estimate the left and right tuning of the resonant peaks inside the PBG of 1D MCPPhC composed of the organic material octane. Fig. 7(a) and (b) show the transmission spectra of 1D MCPPhC of $N = 2$ in the presence of different values of $B = 0T$ to $B = 0.07T$ polarized in RH and LH configurations, respectively. In the case of the RH configuration, the results showed that by increasing B from 0T to 0.07T, the resonant peak became narrower and was shifted to the higher frequency side. However, in the LH configuration, the scenario was entirely different, and the resonant peak was shifted towards the lower frequency side. All the findings are similar to the findings as discussed above.

Thus our findings of the proposed 1D MCPPhCs composed of different organic materials showed how the resonant peaks of unit transmission inside the PBG could be tuned either to the higher or lower frequency side by applying B polarized either in
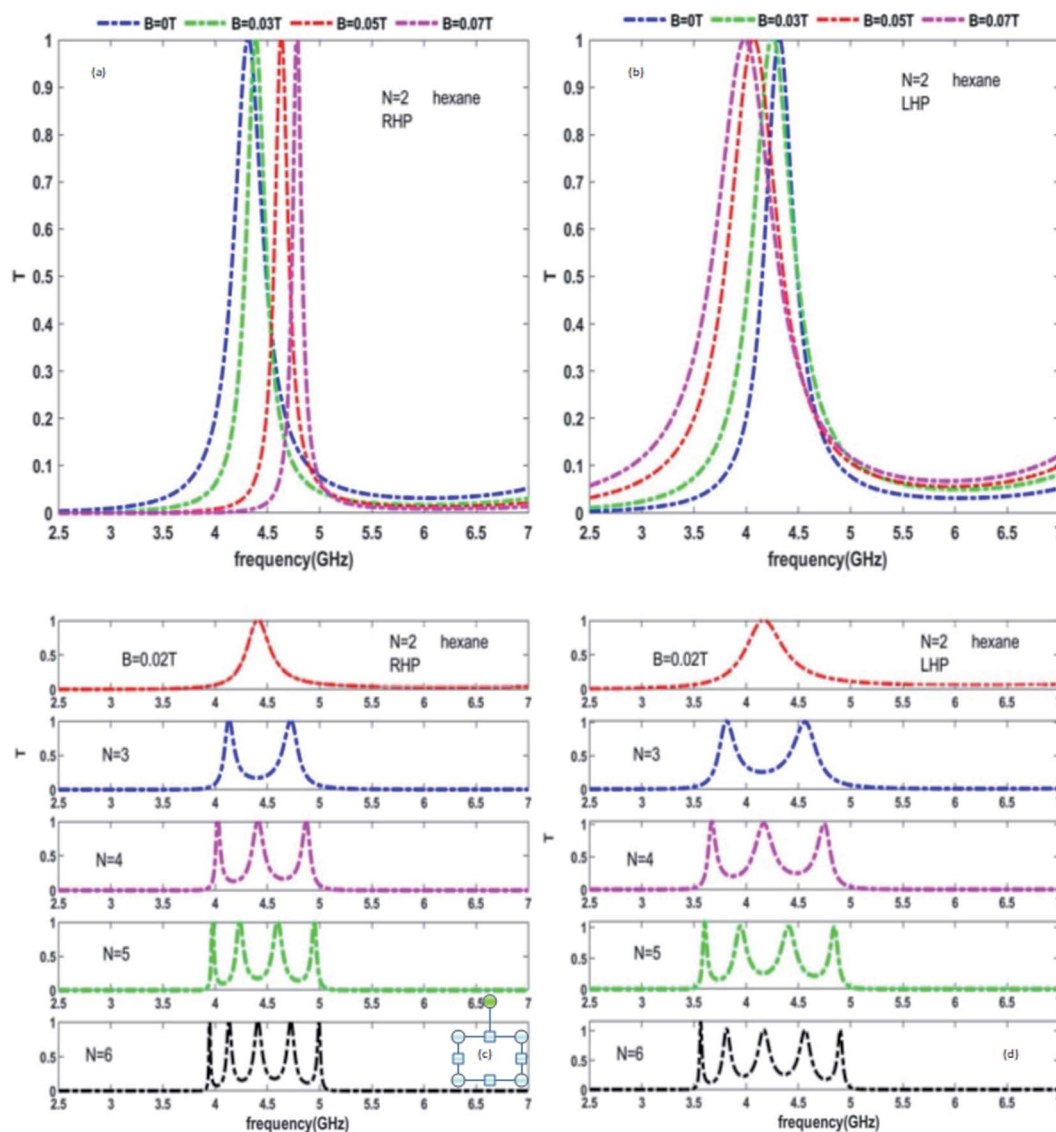
Fig. 5 Effect of the external magnetic field (a and b) and the number of lattice constants (c and d) on the position and number of resonance peaks for both right- and left-hand polarizations plasma layer and when the organic layer is hexane.

a RH or LH configuration. We also studied how N-1 discrete transmission channels of 100%t transmission could be obtained for a given N. These N-1 discrete transmission channels of unit transmission inside the PBG were due to the superposition between the forward decaying and backward decaying evanescent waves, which appeared because MCP does not allow the propagation of incident EMWs of frequencies less than ω_{pe}. These non-propagating incident waves through the MCP generated evanescent waves, which were responsible for the appearance of N-1 transmission channels of 100% transmission. The reason behind the appearance of multiple transmission channels of different central frequencies dependent upon N and B polarized in RH and LH configurations can also be understood by referring to the work of Awasthi in ref. 24. It is important to note that the external magnetic field-dependent shifting features of the resonance peaks was independent of the type of organic materials used to design the particular

MCPPhC. It is worth noting that the red- and blue-shifting of the resonant peaks inside the PBG as a function of B was in agreement with our previous study, where the impact of the external magnetic field on the defect mode position inside the PBG 1D MCPPhC composed of magnetized cold-plasma and a doped semiconductor was studied.[25] The B-dependent tuning of the central frequency of the resonant peaks can be illustrated by the Bragg condition under normal incidence as $2\Lambda = n\lambda$, where Λ is the lattice constant, and n is the effective refractive index of the structure. Thus it can be easily understood with the help of Bragg's condition that under the RH configuration as B increased, the refractive index of the magnetic cold-plasma material also increased, leading to the movement of the resonant peaks towards the higher frequency side. Moreover under the LH configuration, the increase in B resulted in a decrease in the refractive index of the magnetic cold-plasma layer, which
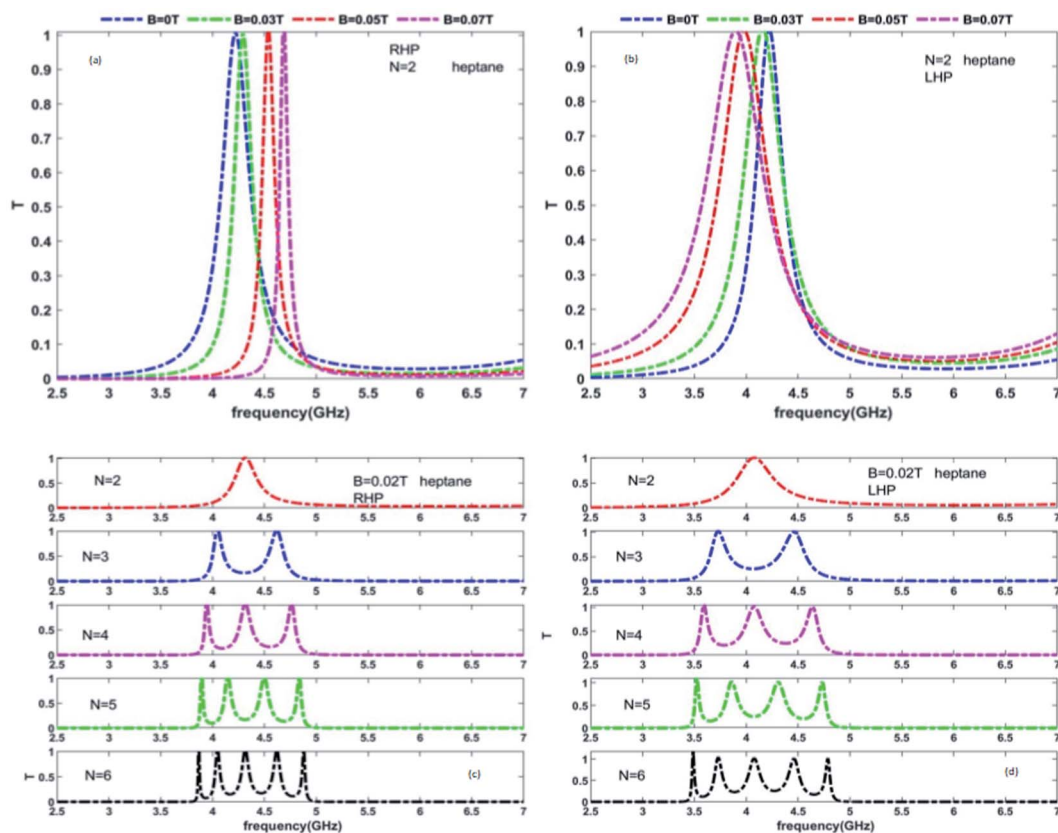
Fig. 6 Effect of the external magnetic field (a and b) and the number of lattice constant (c and d) on the position and number of resonance peaks for both right- and left-hand polarizations plasma layer and when the organic layer is heptane.
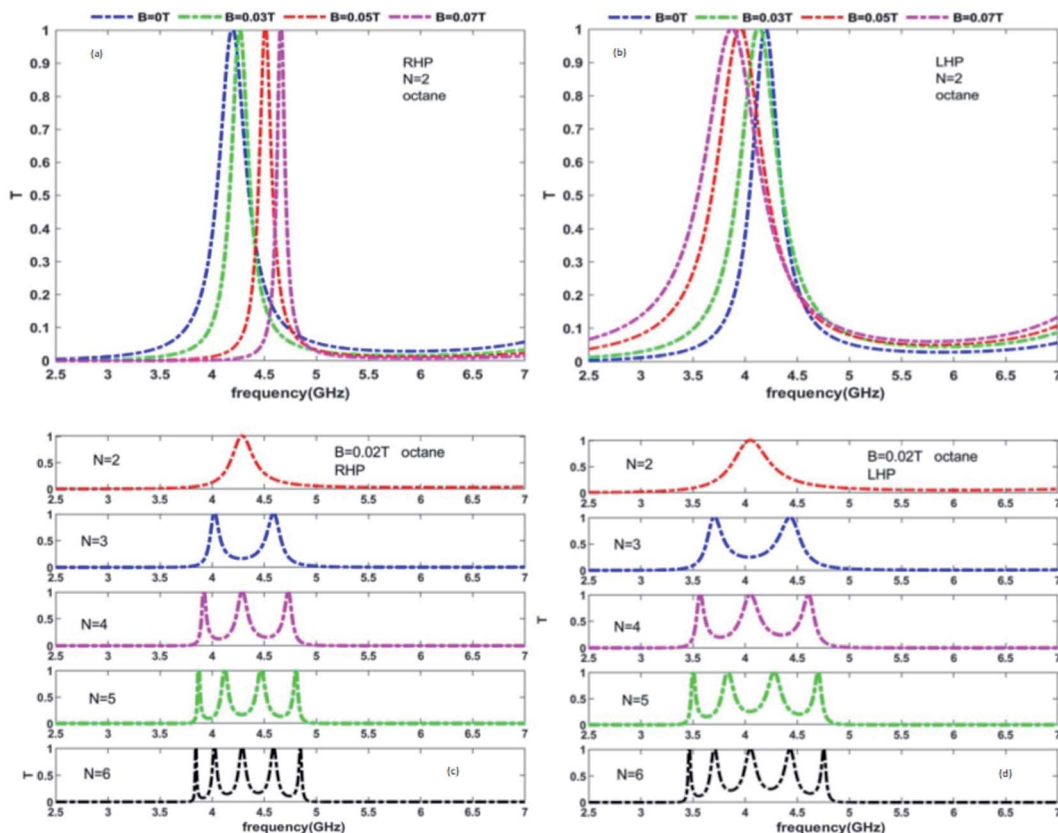

Fig. 7 Effect of the external magnetic field (a and b) and the number of lattice constants (c and d) on the position and number of resonance peaks for both right- and left-hand polarizations plasma layer and when the organic layer is octane

resulted in a shifting of the resonant peaks towards the lower frequency side.

4. Conclusion

In this research work, we theoretically examined the transmission properties of four different 1D PCs composed of four different organic materials (pentane, hexane, heptane, and octane) and magnetic cold-plasma at normal incidence in the presence of B polarized in RH and LH configurations. The simulation results were obtained with the help of TMM and MATLAB software. This study deals with the dependence of the resonant peaks on the period number N and the external magnetic field B polarized in both RH and LH configurations. To the best of our knowledge, such type of research work based on 1D MCPPhC composed of organic materials and magnetic cold-plasma has not been previously reported. Our numerical calculations showed that the resonance peak of unit transmission inside the PBG can be tuned either to the higher or lower frequency side by changing the external magnetic field polarized in RH and LH configurations, respectively. In addition, it was observed that in the case of the right-hand polarized plasma layer, the resonance peak became narrower as the strength of the external magnetic field increased. However, an opposite trend was observed in the case of the left-hand polarized case. Finally, it is worth noting that there existed N-1 number of resonant peaks associated with each 1D MCPPhC for a given period number N. The proposed photonic structures composed of organic materials can be used as a tuneable multichannel narrow filter in the microwave frequency ranges. This may also be beneficial for designing externally tuneable organic material chemical sensors.

Conflicts of interest

The authors declare that there are no conflicts of interest.

References

1 E. Yablonovitch, *Phys. Rev. Lett.*, 1987, **58**, 2059–2062.
2 F. Segovia-Chaves and H. Vinck-Posada, *Physica C*, 2019, **563**, 10–15.
3 M. Abadla and H. Elsayed, *Appl. Opt.*, 2020, **59**, 418–424.
4 S. Li, H. Lin, F. Meng, D. Moss, X. Huang and B. Jia, *Sci. Rep.*, 2018, **8**, 14283.
5 M. N. Armenise, C. E. Campanella, C. Ciminelli, F. Dell'Olio and V. M. N. Passaro VMN, *Phys. Procedia*, 2010, **3**, 357–364.
6 A. H. Aly, F. A. Sayed and H. A. Elsayed, *Appl. Opt.*, 2020, **59**, 4796–4805.
7 A. Panda and P. D. Pukhrambam, *Physica B*, 2021, **607**, 412854.
8 A. Panda, P. Sarkar and G. Palai, *Optik*, 2018, **154**, 748–754.
9 F. Ghasemi, S. R. Entezar and S. Razi, *Laser Phys.*, 2019, **29**, 056201.
10 A. H. Aly, Z. A. Zaky, A. S. Shalaby, A. M. Ahmed and D. Vigneswaran, *Phys. Scr.*, 2020, **95**, 035510.
11 S. K. Awasthi, U. Malaviya and S. P. Ojha, *J. Opt. Soc. Am. B*, 2006, **23**, 2566.
12 H. Hojo H and A. Mase, *J. Plasma Fusion Res.*, 2004, **80**, 89–90.
13 X.-k Kong, S.-b Liu, H.-f Zhang and C.-z Li, *Phys. Plasmas*, 2010, **17**, 103506.
14 S. K. Awasthi, R. Panda and L. Shiveshwari, *Phys. Plasmas*, 2017, **24**, 072111.
15 H. Hojo and A. Mase, *J. Plasma Fusion Res. Ser.*, 2009, **8**, 477–479.
16 Z. A. Zaky, A. Panda, P. D. Pukhrambam and A. H. Aly, *Sci. Rep.*, 2022, **12**, 3754.
17 S. K. Awasthi, R. Panda, A. Verma, P. K. Chauhan and L. Shiveshwari, *Indian J. Phys.*, 2019, **11**, 1–14.
18 A. H. Aly, H. A. Elsayed, A. A. Ameen and S. H. Mohamed, *Int. J. Mod. Phys. B*, 2017, **31**, 1750239.
19 A. H. Aly, S. K. Awasthi, D. Mohamed, Z. S. Matar, M. Al-Dossari and A. F. Amin, *RSC Adv.*, 2021, **11**, 32973–32980.
20 L. Qi and X. Zhang, *Solid State Commun.*, 2011, **151**, 1838.
21 A. H. Aly, S. K. Awasthi, A. M. Mohamed, Z. S. Matar, M. A. Mohaseb, M. Al-Dossari, M. T. Tammam, Z. A. Zaky, A. F. Amin and W. Sabra, *Crystals*, 2021, **11**, 1533.
22 A. H. Aly, S. K. Awasthi, A. M. Mohamed, W. Sabra, M. Mobarak, Z. S. Matar and A. S. Shalaby, *IOP Conf. Ser. Mater. Sci. Eng.*, 2021, **1171**, 012012.
23 H. F. Zhang, S. B. Liu and K. K. Kong, *Phys. Plasmas*, 2012, **19**, 122103.
24 S. K. Awasthi, *Indian J. Phys.*, 2021, **95**, 2785–2795.
25 A. H. Aly and H. A. Elsayed, *J. Mod. Opt.*, 2017, **64**, 871–877.